Friday 2-5

Mechanical Properties of Folded Materials

Brandon Wong

5/13/24
2.671 Measurement and Instrumentation
Friday PM
Dr. Paul Rallager

Abstract

Folded metamaterials offer engineers the potential for lightweight, stiff, impact absorbing, and easily manufacturable options for applications such as the automotive or aerospace industries. A texture analyzer was used to perform compression tests on a series of folded samples of a specific pattern known as the Miura ori pattern, to determine the relationship between the geometric fold angle and the resulting mechanical properties. The properties are found to fit trig functions of the fold angle. Finally, the proportional reduction in mechanical properties from raw paper to folded sample can be extrapolated to predict the properties of similar folded samples made from other materials.

Keywords: Compressive strength, elastic modulus, origami, folded metamaterials, Miura ori pattern

1. Introduction

It is often desirable for materials to be stiff and resist deformations. For example, in the aerospace, aircrafts are often built with "sandwich" composite panels, comprised of some lightweight core (typically aluminum honeycomb) sandwiched by two rigid skins (typically carbon fiber or Kevlar). The structure of this material is advantageous for its strong material properties while remaining lightweight. At the same time, the internal core of the honeycomb composite is able to crumple and absorb impacts if the aircraft were to crash [1,5].

In other times, it is desirable for materials to be compliant and absorb harmful impacts. An example of this is in the packaging industry. Shipping companies that send items via disposable containers benefit from having a packaging material that is cheap, light, and able to resist compressive forces. Sometimes it is also important for the packaging to be able to absorb impacts to protect fragile items inside. Currently, this is usually achieved by cardboard with a corrugated paper core. [9] In both cases mentioned above, it is almost always desirable for materials to be able to have less mass, less volume, and less cost but without compromising on mechanical properties.

While honeycomb and corrugation cores are already effective and well-utilized in their respective industries, origami patterns also present potentially improved mechanical properties for both the aerospace [4-6] and packaging industries [8]. One pattern in particular is known as the Miura ori pattern, whish is composed of periodically alternating parallelograms and can be folded from a flat sheet to create a 3d structure.

Modifying the geometric parameters of the 3d folded structure of the pattern can alter mechanical properties like stiffness and yield strength [8]. One parameter, the "fold angle" between two adjacent faces, is especially important. We seek to determine the relationship between the fold angle and the resulting mechanical properties by compressing folded samples of the Miura ori pattern. Twelve Miura ori samples were folded with varying fold angles, and then the resulting mechanical properties were measured by compressing the samples until failure via a

Texture Analyzer. Ultimately, this data can be used to experimentally validate prior simulation models that have found the theoretical optimal parameters [2,4,6].

2. Background

To begin investigation on the Miura Ori tessellation, a literature review on prior studies relating to the mechanical properties of both this specific pattern as well as materials in general was conducted.

2.1 Miura ori Geometry

The basic repeating cell of the Miura ori pattern is an arrangement of 4 congruent parallelogram faces, which can then be tessellated into an arbitrarily sized lattice arrangement. Figure 1 shows the crease pattern of a Miura ori sample, with one cell highlighted and folded in 3d. Neglecting the thickness of the paper, the geometry of a single cell can be fully defined by 4 parameters: the length and width of the parallelogram, the acute angle of the parallelogram, and a dihedral fold angle θ ranging from 0 (completely folded) to 180 (completely unfolded). With these 4 geometric parameters, the 3d dimensions of the cell can be analytically computed: the cell's height, width, length, transverse area, and bounding box volume [6].

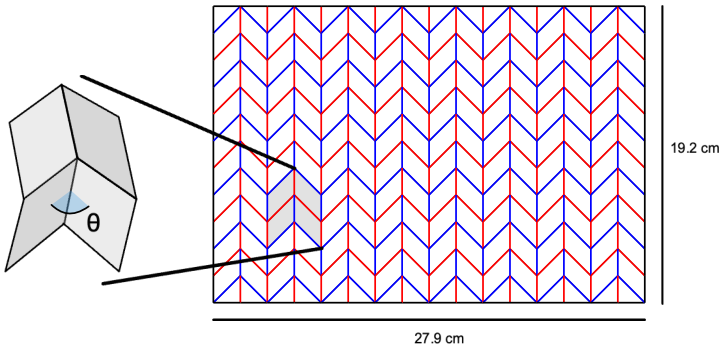

Figure 1: A crease pattern for a sample of the Miura ori pattern, where red lines represent mountain folds and blue lines represent valley folds. The pattern consists of a repeating cell of 4 parallelograms, one of which is highlighted in grey, and partially folded on the left. The fold angle θ refers to the dihedral angle between two faces of the pattern.

2.2 Numerical simulation

The static mechanical properties of the Miura ori pattern have been studied via simulated models by multiple researchers in the past [2,4-6]. Heimbs et.al. simulated compression and shear loads in all three directions and qualitatively calculated the resulting strain-stress curves [5]. They concluded that it behaved similarly to the profiles of other cellular metamaterials like the hexagonal honeycomb. Heimbs et.al also used an Instron machine to perform basic experimental compression tests on a metal Miura ori sample to validate the numerical simulation methods and found that the results were reasonably consistent.

In another numerical study, Kankkunen et.al simulated transverse compressive loads on Miura ori samples with varying geometric parameters and measured the resulting performance factors (strength and stiffness normalized by volume and area of the sample). They found that for some parameters, there exist a range of values to optimize stiffness and buckling resistance, while other parameters did not have local optima. Kankkunen et.al. also took into account the fact that

paper is an orthotropic material (i.e., the mechanical properties of raw paper vary based on direction). As such, the mechanical properties of the Miura ori could vary based on the orientation of the paper it was folded from, but they found that that the stiffness only varied by at most 10% with different fiber orientations [6].

Overall, while the literature presents extensive studies of stiffness, buckling strength, and energy dissipation of the Miura ori pattern under numerically simulated loads, there is still a lack of physical experiments to validate the results of the theoretical models—in particular, to validate Kankkunen et.al's results of the effect of each geometric parameter on the strength and stiffness of the structure. Furthermore, previous experiments have not studied the effect of load rate, plasticity, secondary loading, or factors that affect energy dissipation. While numerical simulation is helpful, it is generally necessary to perform physical testing of a material before using it in real-world applications—especially safety critical applications such as those in the aerospace industry. For these reasons, we wish to perform physical experiments to better understand the material properties of the Miura ori origami pattern.

2.3 Constitutive material

The constitutive material of the samples used in this experiment is paper, which as a raw material is very similar to wood. Wood has a Young's modulus the order of 10 GPa and a density on the order of 1000 kg/m^3. Common engineering metals such as steel alloys usually have a Young's modulus on the order of 100 GPa and densities on the order of 10000 kg/m^3 [10]. Paper is made of a net of fibers, and creating folds in the paper is done by causing permanent breaks in the fibers—this is why it is very difficult to "erase" a crease out of a paper. Metals generally do not share this fiber structure, and thus will often exhibit different mechanical behaviors than those of natural polymers like paper. For this reason, extrapolating the mechanical properties of metals based on the mechanical properties of paper should only be used as a rough estimate. A comparison of the mechanical properties across common materials are plotted on a log-log scale on the Ashby plot in figure 2.

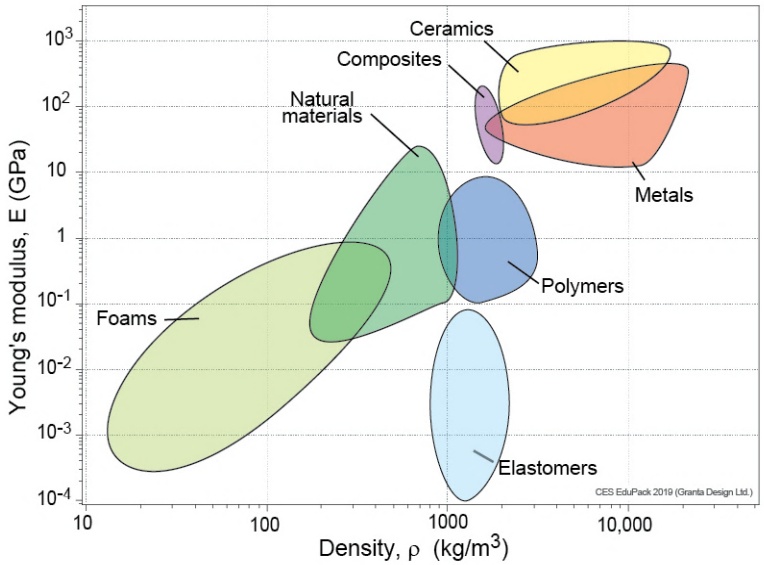

Figure 2: An Ashby plot comparing Young's modulus to density for a variety of different materials. The x-axis is the material density, and the y-axis is the Young's modulus. [10]

This particular Ashby plot shown in figure 2 plots the relationship between the Young's modulus vs density for common materials. The Miura ori pattern reduces both the Young's modulus and the density compared to its constitutive material. The decrease in density can be calculated analytically because it depends purely on the geometry (i.e, it is independent of the material) of the folded sample and thickness of the sheet, whereas the decrease in Young's modulus is one of the parameters that we will calculate in section 4. Like the decrease in density, we expect that the proportional decrease in both Young's modulus will be roughly consistent across materials, allowing us to use paper Miura ori samples to predict the behavior of Miura ori samples of different constitutive materials.

3. Experimental Design

A set of 12 samples were manually folded from standard 8.5x11 inch printer paper using the crease pattern shown in figure 1. All geometric parameters were held constant except for the fold angle θ. The fold angle θ is independent of the crease pattern, and instead is more of an "unfoldedness" angle that can be adjusted after the sample is folded. Using an analytical equation to convert between fold angle and folded sample width, it was possible to accurately set the fold angle for each sample by using a jig of pre-marked lengths. The values of θ ranged from 30 degrees to 105 degrees.

The sample was then placed between the texture analyzer's base plate and a rigid block of wood, as depicted in figure 3. Then, the texture analyzer probe applied up to 500N of compressive force onto the sample and recorded the resulting displacement. It is also worth noting that due to friction between the sample and the base plate/wood block, changes in the sample's transverse area due to its Poisson's ratio are negligible as long as θ does not exceed some threshold. After reaching the load cell's limit of 500N, the probe then returned to allow the sample to release its elastic strain. Finally, the data was exported from the texture analyzer and analyzed in Matlab.

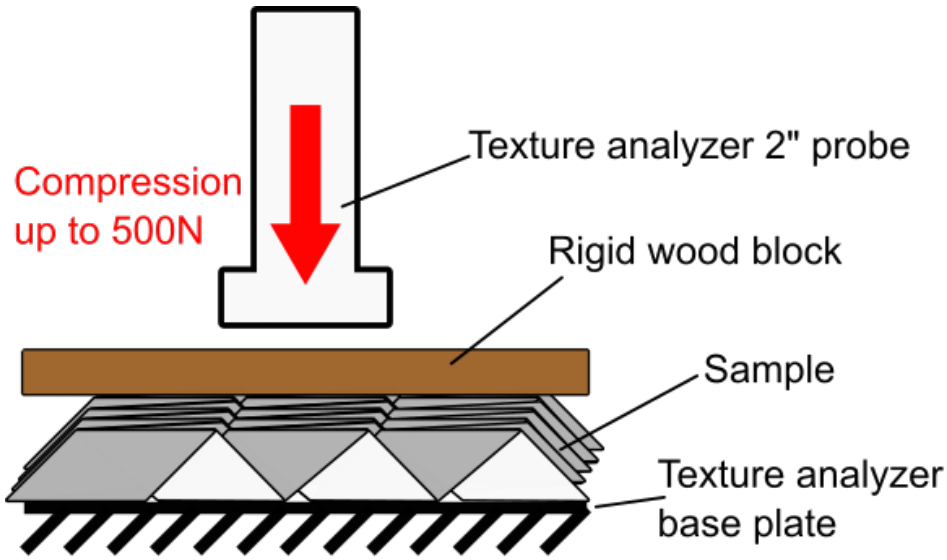

Figure 3: The experimental setup for the texture analyzer. The sample was placed between the texture analyzer's base plate and a rigid block of wood. Then, the texture analyzer probe applied up to 500N of compressive force onto the sample and recorded the resulting displacement.

4. Results and Discussion

The experimental trials described above yielded data that provide evidence towards our research objectives. This data was then analyzed to better understand the mechanical properties of the Miura ori pattern.

4.1 Experimental results

The force-displacement data was exported from the texture analyzer and then plotted as stress-strain curves. This was done by analytically computing the transverse area (for stress calculations) and the initial height of the sample (for strain calculations) based on the sample's fold angle and the dimensions of the unfolded paper. A representative stress-strain curve for various fold angles is shown in the figure 4.

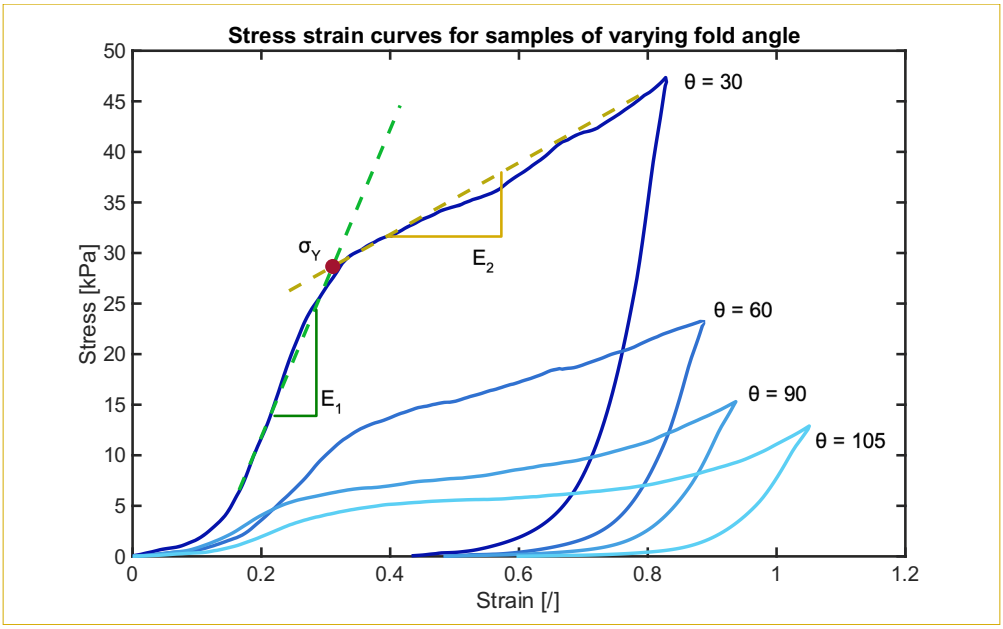

Figure 4: The experimental stress-strain curves for θ = 30, 60, 90, and 105 degrees. These curves were then used to extract the primary Young's modulus (green), yield strength (red), and secondary Young's modulus (yellow) for each curve.

The stress-strain curve appears to have approximately 4 regimes. First, the curve exhibits a "toe" regime where initial strains occur with very low stress. Next is the primary compression regime, where the curve exhibits the maximum stiffness E_1. Upon crossing some yield stress threshold σ_Y, the sample enters a secondary compression regime, where the stiffness E_2 becomes once again roughly linear, although much lower than the primary compression regime. Finally, if the sample continues to be compressed further, it enters a regime where the stiffness once again goes up. This last regime is visible in the samples where θ = 90 and θ = 105, but not for the lower fold angles because the 500N texture analyzer was not able to provide enough force to enter this regime.

Each regime of the stress-strain curve has a hypothesized physical explanation. In the toe regime, the possible explanation is that because the samples were folded by hand, there were slight imperfections in the folded shape and some vertices ended up slightly higher or lower than the rest. Thus the toe regime corresponds to the deformation of the individual vertices in the slight extra height of the sample. In the primary compression regime, the faces and creases are resisting buckling, until the stress reaches a critical amount, and the sample enters the secondary compression regime. In this secondary compression regime, the faces have all buckled but still have some resistance to compression as compressing the sample further essentially requires forming the creases of the crumpled state. In the last regime, the sample has been fully crushed and approaches being mechanically no different than its constituent material (raw paper).

4.2 Data analysis

Given the stress strain curve, we can then numerically extract the mechanical properties E_1, σ_Y, E_2. We define $E_1$to be the steepest slope along the initial linear regime, E_2 to be shallowest slope along the secondary linear regime, and then σ_Y to be the σ value of the point where the two fit lines for E_1 and E_2 intersect as shown in figure 4. Then, using the mass of the samples and the analytical equations for the dimensions of the folded sample based on fold angle, we can normalize the mechanical property values by density to account for the fact that although the samples of higher fold angle were much less stiff and less strong, they also covered more volume. This is also motivated by our overall goal of finding a material that is both strong and lightweight.

Finally, the normalized mechanical property values are fit as trigonometric functions of the fold angle, with 3 parameters for each fit. Although some of plots (especially the yield strength plot) might appear to fit reasonably well to a linear fit, a trig fit makes more physical sense than a linear fit because the independent variable is an angle that ranges from $0 \leq \theta \leq 180$ degrees. Furthermore, the dimensions and shape of the folded sample are all functions of the sine or cosine of θ, so it makes intuitive sense that both the mechanical properties and the densities would also be functions of the sine or cosine of θ. The results with shaded 95% confidence intervals are plotted in the figures below.

The plot for the effect of fold angle on the primary Young's modulus is shown in figure 5.

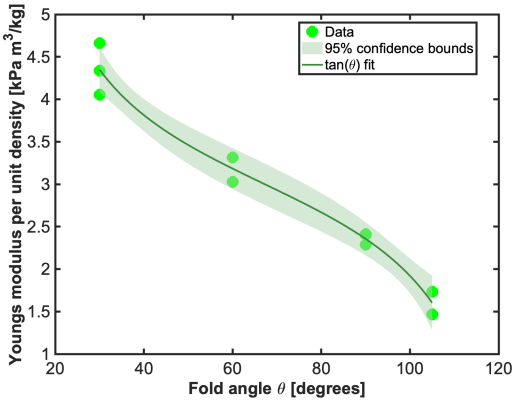

Figure 5: a tan (θ) fit of the primary Young's modulus per unit density as a function of fold angle θ, with 95% confidence interval shaded. There is no locally optimal "sweet spot."

For this fit, a $\tan(\theta)$ makes sense physically and fits the data well within 95% confidence bounds. With all functions of angles, a trigonometric function makes physical sense. As the angle approaches 0, the sample becomes closer to a raw block of paper. It makes sense that this metric, which is modelling the resistance to the onset of buckling and not taking into account direct compression of the material, should approach infinite resistance to buckling for a block of paper.

The plot for the effect of fold angle on the yield strength is shown in figure 6.

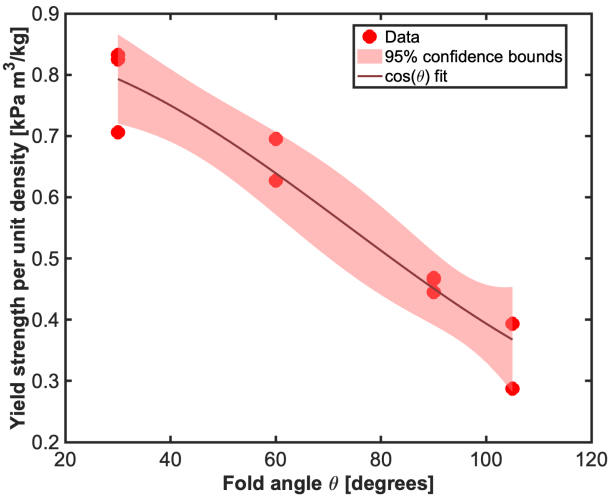

Figure 6: a $\cos(\theta)$ fit of yield strength per unit density as a function of fold angle θ, with 95% confidence interval shaded. There is no local optimum.

Similar to the plot of the primary Young's modulus, it makes mathematical and physical sense to fit the data to a trigonometric function. In this case, $\cos(\theta)$ had the closest fit out of all reasonably possible trigonometric functions. Although cosine functions can have local optimum, it does not fall within the range of values tested, and likely would not be practical to manufacture or use.

The plot for the effect of fold angle on the secondary Young's modulus is shown in figure 7.

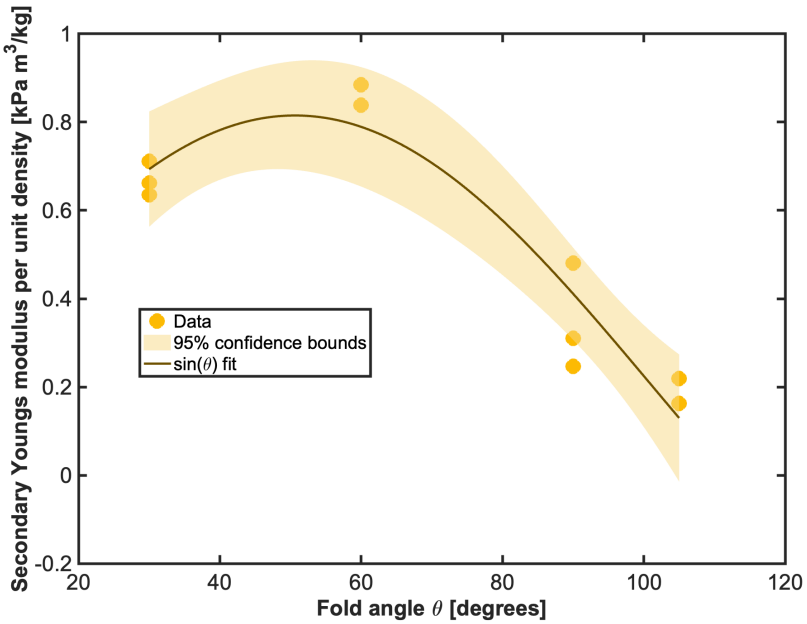

Figure 7: a sin (θ) fit of yield strength per unit density as a function of fold angle θ, with 95% confidence interval shaded. There is a local optimum around θ = 50-60 degrees.

Like the previous two measured mechanical properties, the secondary Young's modulus also fits well to a trigonometric fit. A local optimum for secondary Young's modulus means that this range of angles may not resist the onset buckling (the primary linear regime) as well as lower angles, but it is the optimal angle for maximizing the stiffness per unit density of the material during the buckling process. It makes physical sense to have a local optimum for the secondary Young's modulus. For low angles, the sample is much more dense (decreasing the normalized value) and having its faces start out steeper does not necessarily help to resist buckling.

However, optimizing the secondary Young's modulus is not necessarily the most useful mechanical property to optimize, because once the material reaches the secondary linear regime, it has already passed the yield point and will be sustaining plastic deformation. It is likely more useful to optimize the primary Young's modulus and/or the yield strength to be able to keep the sample in the linear elastic regime for more loading.

4.3 Predictive power for other materials

In most potential real-world applications of folded metamaterials (such as cars or airplanes), using paper as a constituent material would not be very practical. Instead, we would like to use these mechanical properties for samples made of paper to extrapolate the mechanical properties for hypothetical samples made of more conventional engineering materials like metals or polymers.

Using an order of magnitude approximation, raw paper has a Young's modulus similar to wood, on the order of 10 GPa and a density on the order of 1000 kg/m^3 [10]. For paper metamaterial samples of sheet thickness and geometric parameters described in this paper, the Young's modulus is on the order of 10 kPa and the densities are on the order of 10 kg/m^3. Applying these proportions to metals which usually have a Young's modulus on the order of 100 GPa and densities on the order of 10000 kg/m^3 for common engineering metals like steel alloys

[10], we would expect a metamaterial of similar geometry to have a resulting young's modulus on the order of 100 kPa and a density on the order of 100 kg/m^3.

These proportional decreases in density and Young's modulus are plotted in figure 8. Figure 8 features the plot of common engineering materials [10] overlayed with the proportional decrease in Young's Modulus and density for Miura ori samples folded from paper and hypothetically folded from steel.

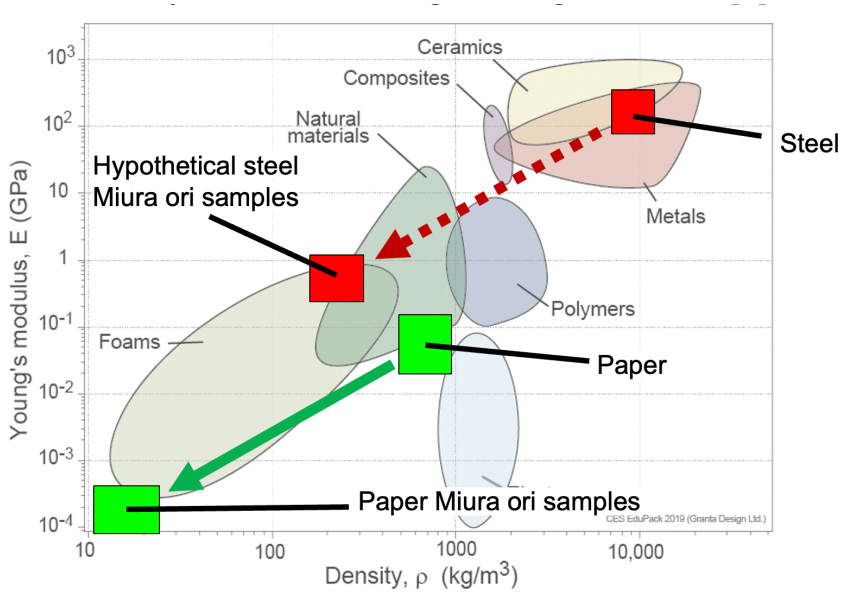

Figure 8: an Ashby plot of Young's modulus vs density for a variety of conventional materials [10]. The proportional decrease from raw paper to the paper Miura ori sample is plotted in green, while the predicted proportional decrease from raw steel to a hypothetical steel Miura ori sample is plotted in red.

This is only a rough approximation and could vary greatly if the thickness of the sheet or other geometric parameters are changed. Additionally, the fact that metals and natural polymers (ie, wood or paper) sometimes have very different mechanical behaviors than metals adds another caveat to the approximation.

4.4 Relation to previous research

One goal of performing physical compression tests on paper samples was to validate or refute the results of numerical simulation done by prior studies. Ignoring the secondary Young's modulus E_2 (which was generally not mentioned in the numerical studies), the experimental plots of E_1/ρ and σ_Y/ρ with respect to fold angle θ generally did not agree with the numerical simulation results of Kankkunen et.al [6]. Notably, one of Kankkunen et.al's conclusions was that there exists a locally optimal value of θ to maximize stiffness or strength per volume, while the experimental results in this paper imply that smaller angles are optimal and there is no sweet spot.

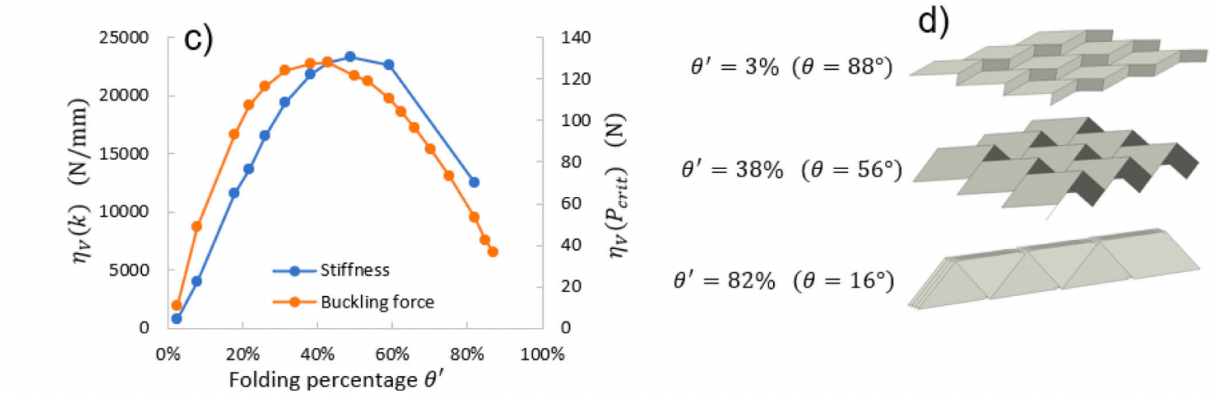

Figure 10: numerical simulation results of Young's modulus * volume vs fold angle. Kankkunen et.al conclude that there is a locally optimal fold angle to maximize Young's modulus. [6] These results are significantly different than experimental results in figure 5.

There are a number of reasonable explanations why the results of prior numerical simulation and the results of physical experiments do not agree. First, the exact computational methods for extracting values for Young's modulus and yield strength were not explicitly explained and could have differed slightly than the methods used in the analysis of this paper. Another important factor is how the material was modelled mathematically, since the mechanics of paper can vary significantly from other materials typically modelled in numerical simulation software. However, the most likely explanation for this discrepancy is that although both the numerical study and this experimental study both were investigating the effects of varying the fold angle θ, the other geometric parameters also could have a significant effect and likely are coupled with θ. If the other parameters such as parallelogram angle or parallelogram height/width ratio were different between the numerical and physical experiments, then it is reasonable that the results would differ.

4.5 Limitations and future extensions

The major limitation with this current method of compressing hand-folded paper samples is the ability to produce a sufficient number of samples that are highly consistent. The samples folded in this project took around 10 minutes per sample, so it would be impractical to manually fold the number of samples that would be needed to thoroughly investigate all of the possible parameters and mechanical properties that could be measured. Additionally, running tests on paper samples provides limited information when the end goal is to make metamaterials out of more practical constituent materials like metals or polymers.

However, if these limitations could be overcome, there is further research that could be done to further study the mechanical properties of origami metamaterials. For example, one broad application of origami metamaterials is for energy absorption as the material crumples, so it would be largely useful to study the toughness of the material and how it responds to different loading rates. Another notable behavior of origami metamaterials like these is that once crushed in the transverse direction, compressing it in one of the other directions can "reset" it to its uncrushed shape due to its positive Poisson's ratio in those directions. However, if compressed again, the stress-strain curve of this secondary compression test would look very different with much lower strength and stiffness. This behavior would also be worth investigating. Finally, for all of these mechanical properties, there are still other geometric parameters beyond the fold angle studied in

this paper that could make a difference. We would like to know how each parameter effects each property in order to fully optimize the geometry of the metamaterial.

5. Conclusions

The experiments in this paper have shown that the mechanical properties (primary Young's modulus, yield strength, and secondary Young's modulus) of the Miura ori pattern depend significantly on the geometric parameters. In fact, the mechanical properties normalized by density were all able to fit to trigonometric functions of the fold angle θ within 95% confidence bounds. The results of these experiment slightly differ from numerical simulation of prior research in that there does not appear to be any optimal value of θ for optimizing the yield strength or primary Young's modulus, although the secondary Young's modulus seems to be optimized when θ is around 50-60 degrees. This is most likely due to the complexity of the geometry and the number of different parameters that all affect the mechanical properties in different ways. In the search for the ultimate metamaterial that can be both strong and lightweight, these experiments provide an order of magnitude predictive model for folded metamaterials that would be made of constitutive materials more practical than paper. Future work includes exploration into the mechanical effect of the other geometric parameters, as well as finding ways to manufacture (and then test) samples folded from metals and materials other than paper. Until then, this paper provides a preliminary experimental understanding of the effect of the fold angle, as well as predicted estimates for other materials to build off of.

Acknowledgments

The author would like to thank Dr. Barbara Hughey and Dr. Paul Ragallar for their guidance and feedback throughout this project.

References

[1] Castanie, Bruno, Christophe Bouvet, and Malo Ginot. 2020. "Review of Composite Sandwich Structure in Aeronautic Applications." Composites Part C: Open Access 1 (August): 100004. https://doi.org/10.1016/j.jcomc.2020.100004.

[2] Chen, Yao, Wangjie Ye, Pan Shi, Ruoqi He, Jinbing Liang, Jian Feng, and Pooya Sareh. 2023. "Computational Parametric Analysis of Cellular Solids with the Miura-Ori Metamaterial Geometry under Quasistatic Compressive Loads." Advanced Engineering Materials 25 (16): 2201762. https://doi.org/10.1002/adem.202201762.

[3] Fischer, Sebastian, Klaus Drechsler, Sebastian Kilchert, and Alastair Johnson. 2009. "Mechanical Tests for Foldcore Base Material Properties." Composites Part A: Applied Science and Manufacturing, Special Issue: CompTest 2008, 40 (12): 1941–52. https://doi.org/10.1016/j.compositesa.2009.03.005.

[4] Heimbs, S., P. Middendorf, S. Kilchert, A. F. Johnson, and M. Maier. 2007. "Experimental and Numerical Analysis of Composite Folded Sandwich Core Structures Under Compression." Applied Composite Materials 14 (5): 363–77. https://doi.org/10.1007/s10443-008-9051-9.

[5] Heimbs, Sebastian, T. Mehrens, Peter Middendorf, Martin Maier, and A. Schumacher. 2007. Numerical Determination of the Nonlinear Effective Mechanical Properties of Folded Core Structures for Aircraft Sandwich Panels.

[6] Kankkunen, Tomi, Jarkko Niiranen, Jarmo Kouko, Miia Palmu, and Kirsi Peltonen. 2022. "Parametric Linear Finite Element Stress and Stability Analysis of Isotropic and Orthotropic Self-Supporting Miura-Ori Structures." Mechanics of Advanced Materials and Structures 29 (27): 5808–22. https://doi.org/10.1080/15376494.2021.1965679.

[7] Liang, Jinbing, Pan Shi, Jian Feng, Pooya Sareh, and Jiansheng Dai. 2023. "Inverse Design of Programmable Poisson's Ratio and in-Plane Stiffness for Generalized Four-Fold Origami." Composite Structures 311. https://doi.org/10.1016/j.compstruct.2023.116789.

[8] Palmu, Miia. 2019. "Folded and Unfolded - Using Tessellation Patterns for Foldable Packaging." https://aaltodoc.aalto.fi/handle/123456789/41206.

[9] Garbowski, Tomasz, and Anna Knitter-Piątkowska. 2022. "Analytical Determination of the Bending Stiffness of a Five-Layer Corrugated Cardboard with Imperfections." Materials 15 (2): 663. https://doi.org/10.3390/ma15020663.

[10] https://www.grantadesign.com/education/students/charts/